



**UNIVERSIDADE ESTADUAL DE CAMPINAS  
SISTEMA DE BIBLIOTECAS DA UNICAMP  
REPOSITÓRIO DA PRODUÇÃO CIENTÍFICA E INTELLECTUAL DA UNICAMP**

**Versão do arquivo anexado / Version of attached file:**

Versão do Editor / Published Version

**Mais informações no site da editora / Further information on publisher's website:**

<https://ieeexplore.ieee.org/document/7165264>

**DOI: 10.1109/EEEIC.2015.7165264**

**Direitos autorais / Publisher's copyright statement:**

©2015 by EEEIC International. All rights reserved.

DIRETORIA DE TRATAMENTO DA INFORMAÇÃO

Cidade Universitária Zeferino Vaz Barão Geraldo

CEP 13083-970 – Campinas SP

Fone: (19) 3521-6493

<http://www.repositorio.unicamp.br>

# Adaptive Saturation System for Grid-Tied Inverters in Low Voltage Residential Micro-Grids

Jakson P. Bonaldo  
UTFPR  
Campo Mourao, Brazil  
jbonaldo@gmail.com

Helmo K. M. Paredes  
Unesp – Univ Estadual Paulista  
Sorocaba, Brazil  
hmorales@sorocaba.unesp.br

Alessandro Costabeber  
University of Nottingham  
Nottingham, UK  
a.costabeber@nottingham.ac.uk

José A. Pomilio  
University of Campinas,  
Campinas, Brazil  
antenor@fee.unicamp.br

**Abstract**—Provision of ancillary services, like power quality improvement is a key to attain higher utilization of multifunctional grid-tied inverter. However, the power quality improvement is mainly limited by the power capacity the grid-tied inverter. This paper explores integration issues of the next-generation intermittent power sources. In particular, two different strategies for enhancing power quality given the residual power capacity of the inverters are developed. One strategy aims to obtain the expected power quality exploiting the dynamic saturation of the inverter rated apparent power and another strategy is based on peak current detection. Both strategies offer the possibility to generate appropriate references for the inner current control loop. The two proposed strategies are compared in performance, and a discussion on their practical implementation for the best performance of the inverters is provided.

**Keywords**—conservative power theory, multifunctional grid-tied inverter, smart micro-grid, power quality.

## I. INTRODUCTION

In recent years, the penetration level of Renewable Energy Sources (RES) in power distribution systems has created increased attention, being an effective solution to environment concerns, a relief for the power system as power is generated and consumed locally (residential applications) and also an essential component of smart micro-grid [1]-[3]. However, the increased number of installations of RES into the grid also brings side effects on the entire distributed network due to the intermittent nature of wind and solar energy, which will as a consequence affect the availability, the reliability, and the quality of the distribution grid.

From another perspective, the intermittent nature of renewable sources can be seen as a chance to optimize the use of power converters when they have residual power capability that is not used for injecting active power generated by the RES. The key component for the connection of RES is the grid-tied inverter (GTI) that acts as the interface between the RES and the utility grid [4]-[6]. Thus, the multifunctional grid-tied inverters have attracted attention in recent years [7]-[9]. In this context, GTI can be used not only as interface of RES but also to provide ancillary services to the network [10]-[12]. In this paper, the ancillary services provided by the GTI are

focused on the improvement of Power Quality (PQ) at the point of common coupling of the GTIs and loads, i.e. using the residual power capacity of the GTI to perform Active Power Filtering functions. However, due to the unpredictable behavior of RESs and loads, the power capacity available in the GTI may be insufficient to perform its primary function, i.e. the injection of the active power generated by the RES, along with the ancillary services. Therefore, this paper presents approaches to deal with the capacity limitation by adapting the level of disturbances compensation leading to the full exploitation of the GTI capability.

## II. FLEXIBLE POWER FACTOR COMPENSATION AND ACTIVE POWER INJECTION INTO THE GRID

In this paper, two dynamic saturation schemes meant to achieve a flexible power factor compensation are discussed. These schemes allow the full utilization of the capability of GTI. In a scenario where the ancillary services are adequately rewarded by the distribution system operator, these strategies would reduce the payback time of the power converter, at the same time improving the PQ of the distribution network. The first proposed strategy is based on GTI apparent power limitation and the second is based on a peak current detection algorithm. These strategies can provide total or partial compensation of the reactive power and harmonic distortion. In this case the compensation aptitude will depend on the residual capacity of the GTI, considering that priority is always given to the maximization of the active power injected into the grid. The two proposed dynamic saturation schemes are based on the power/current orthogonal decomposition of the Conservative Power Theory (CPT) [13]. The basic definitions of the CPT are summarized in Appendix A.

The scheme to generate the reference current of the multifunctional GTI consists of two parts, to generate the two components of the GTI current reference. The first component is the reference current for active power injection from the RES. The second component is the compensation current reference, which is dynamically saturated by a scaling coefficient used to limit the current or apparent power available to use for compensation according to the remaining capacity of the GTI.

When the multifunctional GTI operates as Active Power Filter (APF) and Power Electronic Interface (PEI)

---

This work was supported by the São Paulo Research Foundation (FAPESP) under grants 2011/15884-6; 2013/08545-6; and by CAPES and CNPq.

simultaneously, i.e. injecting active power and compensating disturbances, the active power/current injected into the grid modifies the power factor when measured on the grid side.

Thus, when the RES is operating as pure PEI and is injecting energy into the grid, the resulting power factor on the grid side, is given by:

$$\lambda_G = \frac{P_G}{\sqrt{P_G^2 + A_{na}^2}} = \frac{P - P_{RES}}{\sqrt{(P - P_{RES})^2 + Q^2 + D^2}}. \quad (1)$$

where  $P_G$  is the active power that flows in the grid side including the active power injection ( $P_{RES}$ ) and load active power ( $P$ ). Note that, if the  $P_{RES} = 0$ , the power factor result equal to the load power factor ( $\lambda_G = \lambda$ ). Furthermore, (1) shows that the power factor depends on renewable energy source ( $P_{RES}$ ) and load behaviors ( $P$ ,  $Q$  and  $D$ ). In this case the objective should be compensates all load non-active power ( $A_{na} = \sqrt{Q^2 + D^2}$ ), however, this is not always possible, mainly due to GTI remaining capability which depends on the intermittent nature of solar PV or wind energy.

Hence, in order to provide a reference signal for compensation purpose containing an arbitrary percentage of the non-active power, the instantaneous remaining current (uncompensated) and its RMS value can be given by:

$$i_{na}^* = k i_{na} \Rightarrow I_{na}^* = k I_{na} \quad (2)$$

where  $k$  is a compensation coefficient and can change from 0 to 1 and  $i_{na}$  is the non-active current according to the CPT. In this work, the goal is dynamically adapt this coefficient as a function of the available power capability of the GTI.

Thus, based on uncompensated current (2), the new power factor (fractional compensation), in grid side can be calculated as:

$$\lambda_G^* = \frac{I_G}{\sqrt{I_G^2 + I_{na}^{*2}}} = \frac{P_G}{\sqrt{P_G^2 + A_{na}^{*2}}} \quad (3)$$

It should be noted that, due to the property of orthogonality between the current components, the power factor can be adjusted, in any percentage, thus providing flexibility with respect to the objectives compensation. Therefore, from (1), (2) and (3) the compensation coefficient ( $k$ ) is given by:

$$k = \frac{\lambda_G}{\lambda_G^*} \sqrt{\frac{1 - \lambda_G^{*2}}{1 - \lambda_G^2}} \quad (4)$$

Thus, for a given (desired) value of the power factor ( $\lambda_G^*$ ) imposed to meet a specific standard, the value of compensation coefficient ( $k$ ) is easily obtained by (4). The range of  $\lambda_G^*$  values may vary between  $\lambda_G$  and 1. Note that for  $\lambda_G^* = 1$ , the compensation coefficient results zero ( $k = 0$ ). In this case, from (2), the non-active current reference also results zero ( $I_{na}^* = 0$ ). This means that the GTI compensates all non-active power resulting in a current on the grid side in phase and with the same waveform of the PCC voltage, exactly as in the case of resistive load. Therefore, in order to provide a flexible compensation and active power injection, the reference signal generator that contains an arbitrary percentage of the undesired components of the current can be expressed as a function of compensation coefficient, as:

$$i_{comp}^* = i_{na} - i_{na}^* = i_{na}(1 - k) \quad (5)$$

Therefore, the instantaneous multifunctional GTI reference current is given by:

$$i_{inv}^* = i_{RES}^* + i_g^* - i_{comp}^* \quad (6)$$

where  $i_g^*$  is the reference which keeps the DC bus voltage regulated and  $i_{RES}^*$  is the reference current to transfer the energy generated into the grid, which is determined by the equivalent conductance ( $G_{DG}$ ), which is given by:

$$i_{RES}^* = \frac{P_{RES}}{V_{PCC}^2} \cdot v_{PCC} = G_{DG} \cdot v_{PCC} \quad (7)$$

This decomposition is a general representation to include the case where an energy storage is coupled with the RES. Otherwise, the current reference  $i_g^*$  automatically includes the power transfer from the RES to the grid. It should be underlined that, when there is injection of active power into the grid and there is no adequate choice of the desired power factor, the non-active power ( $A_{na}$ ) associated with load disturbances could become greater than the available power of the GTI. Therefore, if one desires full compensation, the overload protections of the GTI would be triggered, causing GTI shutdown. The block diagram to generate the instantaneous reference current of the multifunctional GTI is depicted in the Fig. 1.

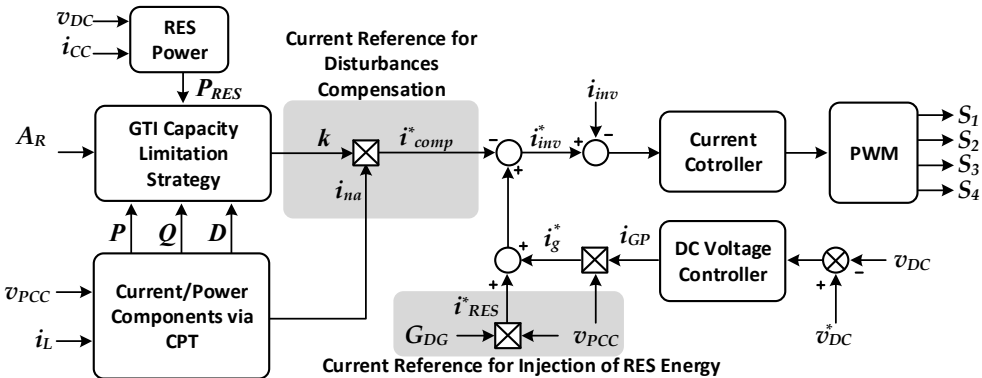


Fig. 1. Control system with and without dynamic saturation of apparent power of the multifunctional GTI.

### III. STRATEGIES TO DEAL WITH GTI LIMITED CAPACITY

As mentioned earlier, two strategies to deal with capacity constraints of the GTI are provided in this section.

#### A. Dynamic saturation of the GTI apparent power

Due the intermittent nature of the RES, the power available ( $A_A$ ) in the GTI is the portion that is not used to inject active power from the RES ( $P_{RES}$ ) into the grid, and can be given by:

$$A_A = \sqrt{(A_R)^2 - (P_{RES})^2} \quad (8)$$

where  $A_R$  is the rated apparent power of the GTI.

A simple way to prevent the GTI processing of a power amount greater than its rated capacity is performing a partial compensation of the non-active power. In this case the assumption is that the partial compensation does not exceed the GTI available power ( $A_A$ ). Thus, (3) can be automatically adjusted to achieve the highest possible level of compensation according the remaining capacity of GTI. Thus, the power factor in grid side becomes

$$\lambda_{G-a}^* = \frac{P_G}{\sqrt{P_G^2 + (A_{na} - A_A)^2}} = \frac{P_G}{\sqrt{P_G^2 + A_{na-nc}^2}} \quad (9)$$

where  $A_{na-nc}$  is the amount related to non-active power which is not compensated, due to lack capacity of the GTI. Note that, in the case where the power available in the GTI is larger than the load non-active power ( $A_A \geq A_{na}$ ), the power factor on grid side result unitary, meaning that the residual power is enough to compensate all the non-idealities of the load. Cases where this condition is not satisfied, result in partial compensation of the power factor. Therefore, the compensation coefficient (4) and the reference signal generator (5) are actualized automatically according (9). The flowchart depicted in Fig. 2 summarizes the steps to obtain the optimal compensation coefficient. Please note the limited complexity of the saturation scheme obtained applying the theoretical framework provided by the CPT.

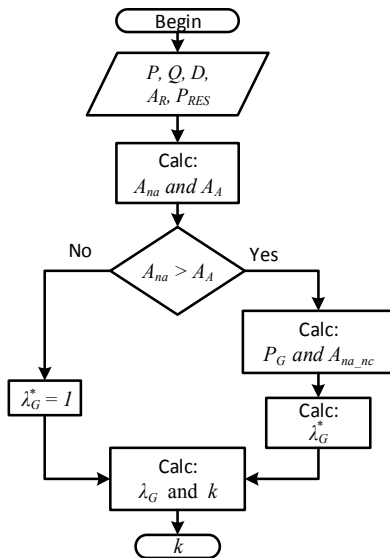


Fig. 2. Flowcharts for dynamic saturation of the apparent power processed by GTI.

#### B. Dynamics saturation of the GTI peak current

Depending on the characteristics of the GTI, limiting the power may be insufficient to keeps GTI operation inside a safety region, since peaks of current throughout the GTI could violate its current rating. This kind of situation may happens when the multifunctional GTI is required to compensate a nonlinear load, which could have current peaks much larger than its RMS current. Therefore, another alternative approach to capacity limitation is discussed in this section. In this strategy, the instantaneous output current of GTI is dynamically limited. Since the main function of the GTI is to extract the maximum energy of the RES to inject it into the grid, the active current is maintained without any limitation. Therefore, the alternative to saturate the GTI peak current is to limit the reference current related to compensation the reactive and harmonic current, i.e., non-active current.

The algorithm used to perform current limitation is shown in Fig. 3. Note that, the limitation strategy operates generating a dynamic compensation coefficient ( $k$ ) that is adapted according to the GTI residual current capacity. Finally, the reference current ( $i_{comp}^*$ ) for non-active current compensation can be generated. The peak detector is used to obtain the ideal maximum amplitude of the reference current,  $i_{inv\_full}^*$ , which is the current required to fully compensate the load power factor at the same time providing the active power injection from the RES and is calculated as:

$$i_{inv\_full}^* = i_{RES}^* + i_g^* - i_{na} \quad (10)$$

It is worth to underline that the reference  $i_{inv\_full}^*$  would perform power injection and full compensation of disturbances if it was applied as the current reference for the GTI. However, as shown in Fig. 3, the current reference is given by:

$$i_{inv}^* = i_{RES}^* + i_g^* - i_{comp}^* = i_{RES}^* + i_g^* - k \cdot i_{na} \quad (11)$$

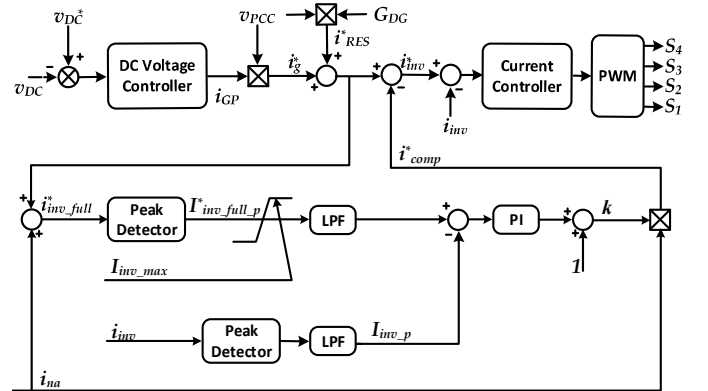


Fig. 3. Proposed scheme for GTI current saturation.

The value of the detected peak is given by  $i_{inv\_full\_p}^*$ . If this value is larger than the maximum current peak allowed in the GTI ( $I_{inv\_max}$ ), it is saturated and a low-pass filter is used to mitigate fluctuations in the peak value of the GTI current and it is compared with the peak value of the current that actually flows through the GTI ( $i_{inv\_p}$ ). Finally, the error is processed by a proportional integral controller, resulting in the compensation coefficient ( $k$ ). In other words, the control law

dynamically calculates the compensation coefficient ( $k$ ) which determines how much of non-active current can be compensated ( $i_{comp}^*$ ). This action ensures that the GTI will work below rated current. The peak of rated current is given by  $I_{inv\_max}$ . The control loop has a saturator to ensure that the reference current do not exceed the rated current of GTI while the dynamic saturation strategy determines the amount of non-active current (harmonic and reactive current) which will be compensated. Note that, if  $i_{inv\_full\_p}^* < i_{inv\_max}$ , the PI output is annulled, resulting  $k = 1$ , which leads to the total compensation of the non-active current.

#### IV. SIMULATION RESULTS

The system under investigation is shown in Fig. 4. A LCL filter is used as an interface between the grid and the GTI [14]. Table I describes the main parameters of the system.

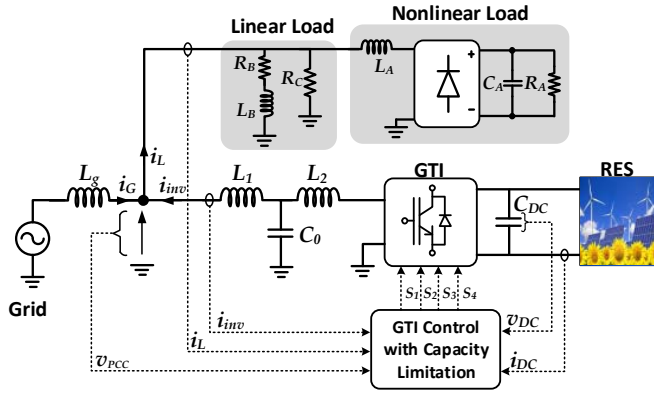


Fig. 4. Typical multifunctional GTI.

TABLE I. PARAMETERS OF THE INVESTIGATION SYSTEM.

Parameter	Value	Parameter	Value
Grid	127 V / 60 Hz	$L_g, R_g$	0.2 mH; 0.1 $\Omega$
$P_{RES}$	1.8 kW	$L_B, R_B$	60 mH; 4 $\Omega$
$L_A$	1 mH	$R_C$	100 $\Omega$
$R_A$	25 $\Omega$	$C_A$	1 mF
$L_1 = L_2$	0,5 mH	$C_0$	3 $\mu$ F

Both strategies for current and power limitation use a current controller to enforce the multifunctional GTI to synthesize the calculated current reference. A proportional resonant plus harmonic controller (PR+HC) shown in (12) is used to perform this function [15]. A proportional integral controller (PI), which is shown in (13), is used to keep the DC voltage regulated at the desired value. The value of the controllers parameters are shown in Table II. Simulations of each limitation strategy applied to the test system of Fig. 4 are performed in the following subsections.

TABLE II – CONTROLLERS PARAMETERS.

$K_c = 0.95$	$K_{IPR} = 100$
$\omega_{cPR} = 5[\text{rad/s}]$	$\omega_o = 377[\text{rad/s}]$
$K_{P\_DC} = 2.2$	$K_{I\_DC} = 49$

$$G_C(s) = K_C + \sum_{h=1,3,5,\dots,15} \frac{2K_{IPR}\omega_{cPR}s}{s^2 + 2\omega_{cPR}s + (h\omega_o)^2}, \quad (12)$$

$$PI_{DC}(s) = K_{P\_DC} + \frac{K_{I\_DC}}{s} \quad (13)$$

#### A. Performance of multifunctional GTI with apparent power saturation strategy

In this case, the goal is to show that the apparent power processed by the GTI does not exceed its rated capacity while providing APF ancillary services. The rated capacity of the GTI is supposed to be  $A_R = 2\text{kVA}$ . Firstly, the multifunctional GTI is OFF. At  $t = 0.5\text{s}$  the multifunctional GTI is turned ON for inject only active power into the grid (without any compensation function). At  $t = 1\text{s}$ , the compensation function is activated for full non-active current compensation, without enabling the saturation strategy. Finally, at  $t = 1.5\text{s}$  the proposed saturation strategy is activated. The system operation is described by making reference to the apparent, active, reactive, distortion powers and power factor at grid, load and multifunctional GTI side.

Fig. 5 depicts the performance of the multifunctional GTI on the different operating conditions. It can be seen that when the inverter operates as a multifunctional GTI (PEI + APF) compensating full non-active power ( $0.5\text{s} < t < 1\text{s}$ ), the apparent power of the inverter is larger than its rated apparent power ( $A_{GTI} = 2.247\text{kVA} > 2\text{kVA} = A_R$ ).

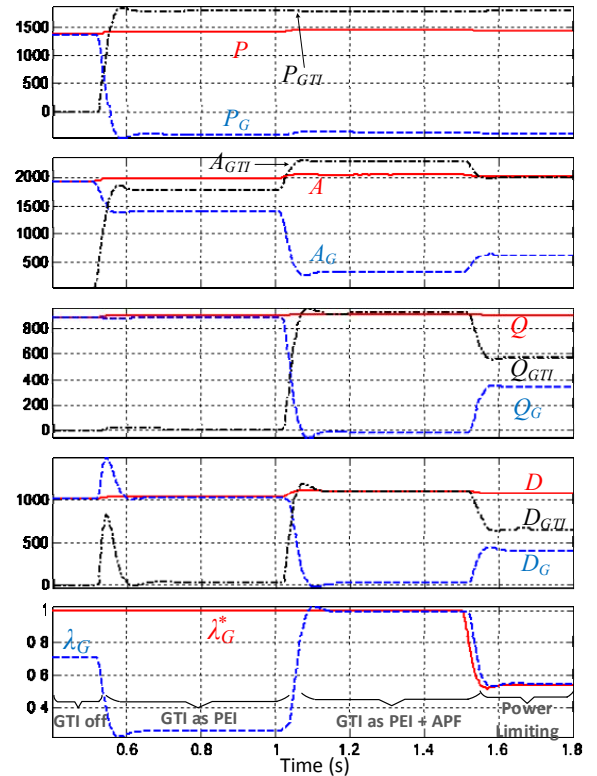


Fig. 5. Apparent, active, reactive, distortion power and power factor dynamics for multifunctional GTI for different operating conditions.

In this situation, the reactive power and harmonics of the grid goes to zero and all reactive power and harmonics of the load is supplied by the multifunctional GTI. However, this power profile could not be sustained, because the inverter

operates out of its rated capacity. Instead, in the interval where the saturation of the control loop is enabled ( $t > 1.5s$ ), the apparent power of the inverter is properly saturated. The dynamic saturation scheme prevents the full non-active power compensation thereby the GTI apparent power works in the limits of its capacity ( $A_{GTI} = A_R = 2 \text{ kVA}$ ).

### B. Performance of multifunctional GTI with peak current saturation strategy

Fig. 6 and Fig. 7 show the performance of the multifunctional GTI with peak current saturation scheme. The system was simulated following the same operation conditions of the previous strategy.

Fig. 6 shows the instantaneous current ( $i_{inv}$ ), peak current ( $i_{inv\_p}$ ) and the maximum current peak allowed in the GTI ( $i_{inv\_max}$ ). In this case,  $i_{inv\_max}$  is supposed to be 30 A. When the multifunctional GTI operates only as PEI ( $t > 0.5s$ ) injecting energy into the grid,  $i_{inv\_p} = 20A$  ( $P_{GTI} = P_{RES} = 1.8 \text{ kW}$ ). The power factor in grid side is low ( $\lambda_G = 0.27$ ), because the grid supplies the reactive and harmonic current demanded by the load. With the available capacity, at  $t = 1s$ , the multifunctional GTI starts the compensation of harmonics and reactive current. It can be seen that to make the total compensation of the non-active current ( $\lambda_G = 1$ ), the multifunctional GTI is required to synthesize a current waveform with 40A of peak value. However, this value is bigger than the maximum current peak allowed ( $i_{inv\_p} = 40 \text{ A} > i_{inv\_max} = 30 \text{ A}$ ). Therefore, the peak current saturation strategy begins to act at  $t = 1.5s$ . Note that, the compensation capability was reduced ( $\lambda_G = 0.69$ ), ensuring that the reference current of the multifunctional GTI does not exceed the current limit ( $i_{inv\_p} = i_{inv\_max} = 30 \text{ A}$ ).

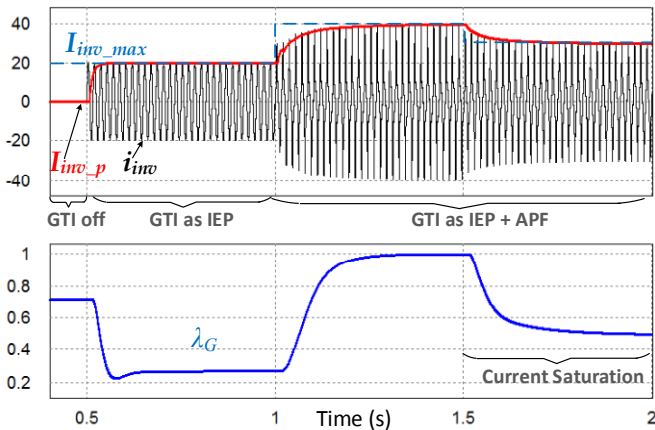


Fig. 6. Dynamics saturation of the multifunctional GTI output current for different operating conditions.

The behavior of powers is presented in Fig. 7. Note that, the apparent power processed by the multifunctional GTI when its current is not being limited is  $A_{GTI} \approx 2.3 \text{ kVA}$ . When the peak current saturation strategy is acting ( $t > 1.5 \text{ s}$ ) the peak current is limited to  $i_{inv\_p} = 30 \text{ A}$ , as shown in Fig. 6. Therefore, the apparent power processed by GTI during current saturation is  $A_{GTI} \approx 1.95 \text{ kVA}$ . Hence, this fact might suggest that a GTI with rated capacity of 2 kVA could be used as the multifunctional device. However, this assumption is not true,

since the maximum current peak allowed in a 2 kVA GTI is  $i_{inv\_max} = 22.5 \text{ A}$ .

On the other hand, a GTI which allows a peak current of 30 A would need to be rated to  $A_R = 2.69 \text{ kVA}$ , exactly like the multifunctional GTI used to obtain the results shown in Fig. 6 and Fig. 7. It is worth to underline that, when operating as APF, the GTI current is not sinusoidal, and the overcurrent tripping (operation of the peak current saturation strategy) is caused by the peaks due to the harmonic content of the load current.

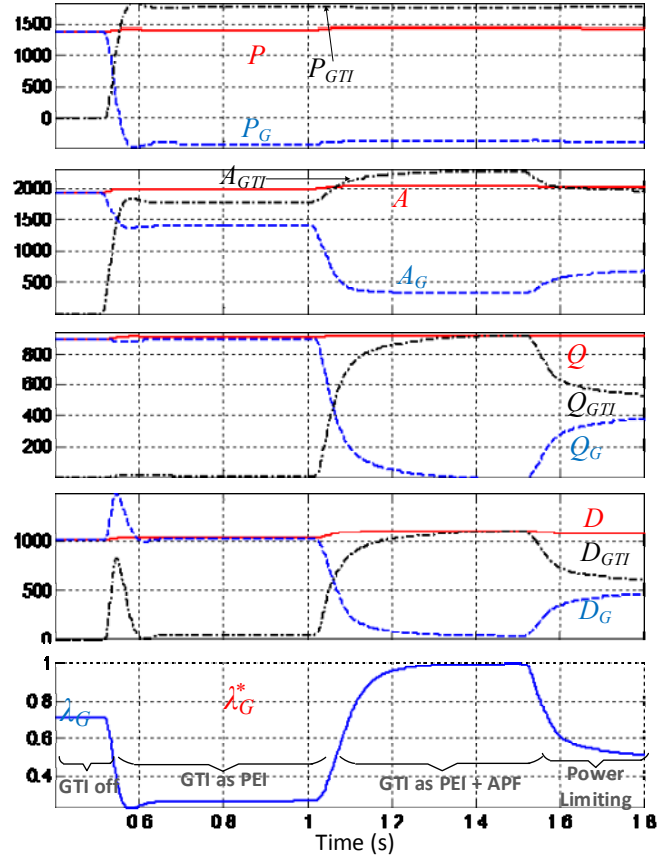


Fig. 7. Powers behavior of the dynamics saturation of the multifunctional GTI output current for different operation condition.

## V. CONCLUSION

This paper proposed two dynamic saturation strategies to allow the full use of the capacity of GTIs, even considering variable loads and unpredictable amounts of power generation by the RES:

- The first strategy is based on the apparent power available in the GTI, which is not used to inject the active power generated by RES into the grid. Since there is power capacity available in the GTI, it is used to improve the power factor at the PCC.
- The second strategy aims at limiting the peak current that flows throughout the GTI. Therefore, if the current becomes larger than the maximum limit allowed by the GTI, the compensation of disturbances is automatically

limited and the GTI current is kept within the limits, avoiding undesired tripping.

Such situation leads to a partial compensation of disturbances that improves the PQ at point of connection of the GTI. Both strategies allow the full exploiting of GTI capacity. However, the current peak based strategy ensures the operation of GTI without exceeding current and power limits. Therefore, this may work like a worst case approach, ensuring safest operation of the GTI. Furthermore, the proposed control strategy can be easily implemented in a commercial GTI as a standardized functions.

#### REFERENCES

- [1] G. Venkatarammann, C. Marnay, "A Large Role for Microgrids: Are Microgrids a Viable Paradigm for Electricity Supply Expansion?" *IEEE power& Energy Magazine*, pp. 78-82, May/June 2008.
- [2] G. T. Heydt, "The next generation of power distribution systems," *IEEE Trans. Smart Grid*, vol. 1, no. 3, pp. 225-235, Nov. 2010.
- [3] G. Venkatarammann, C. Marnay, "A Large Role for Microgrids: Are Microgrids a Viable Paradigm for Electricity Supply Expansion?" *IEEE power& Energy Magazine*, pp. 78-82, May/June 2008.
- [4] Riming Shao; Kaye, M.; Liuchen Chang, "Advanced building blocks of power converters for renewable energy based distributed generators," *Power Electronics and ECCE Asia (ICPE & ECCE)*, 2011 IEEE 8th International Conference on, vol., no., pp.2168-2174, May 30 2011-June 3 2011.
- [5] J.M. Carrasco, L.G. Franquelo, J.T. Bialasiewicz, E. Galvan, R.C.P. Guisado, M.A.M. Prats, J.I. Leon, N. Moreno-Alfonso, "Power-Electronic Systems for the Grid Integration of Renewable Energy Sources: A Survey", *IEEE Transactions on Industrial Electronics*, vol.53, no.4, pp.1002,1016, June 2006.
- [6] B. N. Alajmi, K. H. Ahmed, G. P. Adam, B. W. Williams, "Single-Phase Single-Stage Transformer less Grid-Connected PV System," *IEEE Transactions on Power Electronics*, vol.28, no.6, pp.2664-2676, June 2013.
- [7] R. Bojoi, L. R. Limongi, D. Roiu, A. Tenconi, "Enhanced power quality control strategy for single-phase inverters in distributed generation systems," *IEEE Trans. on Power Electronics*, vol. 26, no. 3, pp. 798-806, Mar 2011.
- [8] Y. W. Li, D. M. Vilathgamuwa, and P. C. Loh, "A grid-interfacing power quality compensator for three-phase three-wire microgrid applications", *IEEE Trans. Power Electron*, vol. 21, no. 4, pp. 1021-1031, Jul. 2006.
- [9] Y. Yang, F. Blaabjerg, H. Wang and M. G. Simões, "Power Control Flexibilities for Grid-Connected Multi-Functional Photovoltaic Inverters", in *Proc. of International Workshop on Integration of Solar Power into Power Systems*, November 2014.
- [10] S. Munir, Y. W. Li, "Residential Distribution System Harmonic Compensation Using PV Interfacing Inverter," *IEEE Transactions on Smart Grid*, vol.4, no.2, pp.816,827, June 2013.
- [11] S. Dasgupta, S. K. Sahoo, and S. K. Panda, "Single-phase inverter control techniques for interfacing renewable energy sources with microgrid—Part I: Parallel-connected inverter topology with active and reactive power flow control along with grid current shaping," *IEEE Trans. Power Electron*, vol. 26, no. 3, pp. 717-731, Mar. 2011.
- [12] D. Ahmadi, W. Jin, "Online Selective Harmonic Compensation and Power Generation With Distributed Energy Resources", *IEEE Transactions on Power Electronics*, vol.29, no.7, pp.3738,3747, July 2014.
- [13] P. Tenti, H. K. M Paredes, P. Mattavelli, "Conservative Power Theory, a Framework to Approach Control and Accountability Issues in Smart Microgrids," *IEEE Trans. on Power Electronics*, vol.26, no.3, pp.664-673, Mar 2011.
- [14] Chiang, P. L.; Holmes, D.G., "Analysis of multiloop control strategies for LC/CL/LCL-filtered voltage-source and current-source inverters,"

Industry Applications, *IEEE Transactions on*, vol.41, no.2, pp.644,654, March-April 2005

- [15] Yepes, A.G.; Freijedo, F.D.; Lopez, O.; Doval-Gandoy, J., "Analysis and Design of Resonant Current Controllers for Voltage-Source Converters by Means of Nyquist Diagrams and Sensitivity Function," *Industrial Electronics*, *IEEE Transactions on*, vol.58, no.11, pp.5231-5250, Nov. 2011.

#### APPENDIX A

##### CURRENT AND POWER COMPONENTS OF THE CPT

According the Conservative Power theory (CPT) in any single phase systems, the PCC current can be decomposed into:

$$i = i_a + i_r + i_v = i_a + i_{na}. \quad (A.1)$$

where  $i_a$  is the active current,  $i_r$  is the reactive current,  $i_v$  is the void current and  $i_{na}$  is the non-active current.

- The *active current* is:

$$i_a = \frac{\langle v, i \rangle}{V^2} v = \frac{P}{V^2} v = G_e v. \quad (A.2)$$

such that  $V$  is the RMS value (Euclidean norm) of the voltage and parameter  $G_e$  is the equivalent conductance. In (2), the operation  $\langle \cdot, \cdot \rangle$  represents the internal product between the voltage and current which stands for the active power ( $P$ ).

- The *reactive current* is:

$$i_r = \frac{\langle \hat{v}, i \rangle}{\hat{V}^2} \hat{v} = \frac{W}{\hat{V}^2} \hat{v} = B_e \hat{v}, \quad (A.3)$$

such that  $\hat{v}$  is the unbiased voltage integral and parameter  $B_e$  is the reactivity equivalent.

- The *void current* is:

$$i_v = i - i_a - i_r. \quad (A.4)$$

By definition, all the components of current defined earlier are orthogonal to each other. Therefore, the total current at the PCC is given by:

$$I^2 = I_a^2 + I_r^2 + I_v^2 = I_a^2 + I_{na}^2. \quad (A.5)$$

Therefore, the apparent power can be decomposed as:

$$A^2 = V^2 I_a^2 + V^2 I_r^2 + V^2 I_v^2 = V^2 I_a^2 + V^2 I_{na}^2 \quad (A.6)$$

where:

- $V I_a = P$  is the active power
- $V I_r = Q$  is the reactive power
- $V I_v = D$  is the void power (distortion power)
- $V I_{na} = A_{na}$  is the non-active power

Finally, the power factor may be calculated as following:

$$\lambda = \frac{P}{A} = \frac{P}{\sqrt{P^2 + Q^2 + D^2}} = \frac{P}{\sqrt{P^2 + A_{na}^2}} \quad (A.7)$$